Electronic Supplementary Information

A new disulfide Schiff base as versatile "OFF-ON-OFF" fluorescent-colorimetric chemosensor for sequential detection of CN− and Fe3+ ions: Combined experimental and theoretical studies

Fariba Nouri Moghadam, [a] Mehdi Amirnasr, * [a] Kiamars Eskandari, [a] Soraia Meghdadi [a]

[a] *Department of Chemistry, Isfahan University of Technology, Isfahan 8415683111, Iran*

*Corresponding author Tel.: +98-31-3391-3264; Fax.: +98-31-3391-2350.

E-mail address: amirnasr@cc.iut.ac.ir (M. Amirnasr)

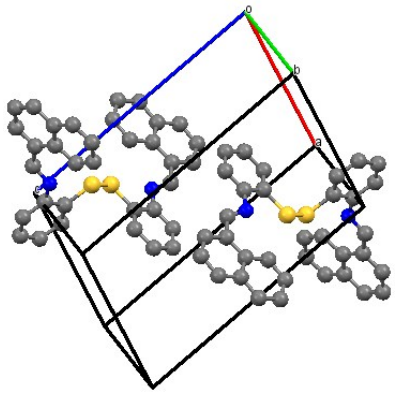

Fig. S1. Unit cell structure of **L**. The molecule crystallizes in a centro-symmetric triclinic space group, $P\bar{1}$ with $Z = 2$.

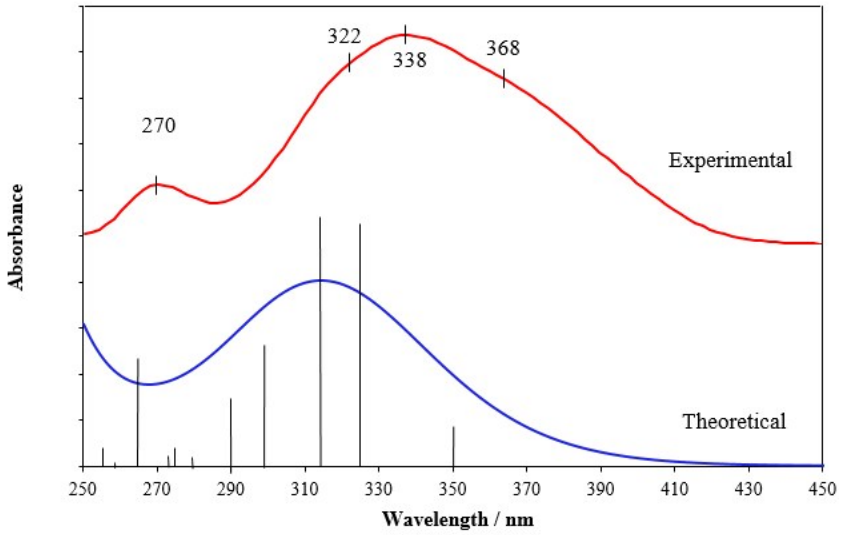

Fig. S2. The comparison of the experimental (red) and calculated (blue) absorption spectra of **L** in DMSO solution.

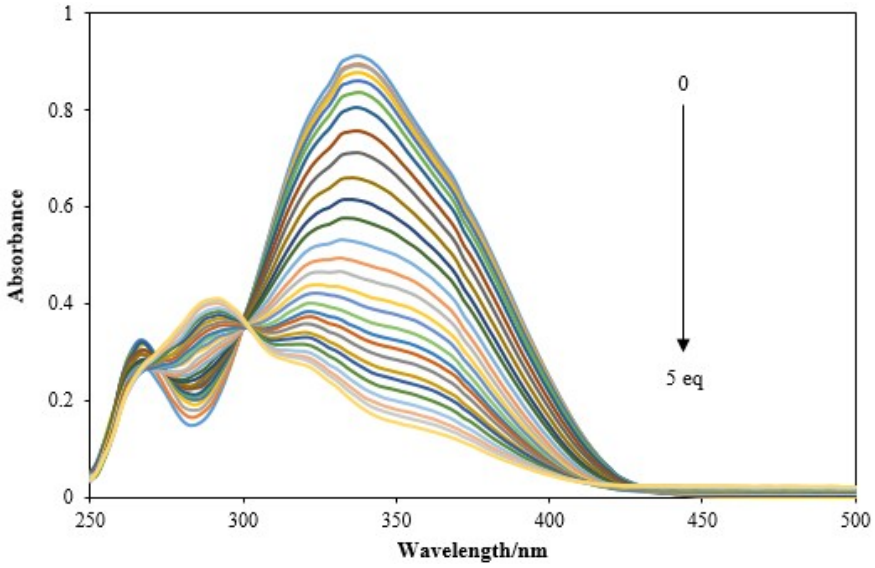

Fig. S3. Changes in the UV-vis spectrum of **L** (30 μM) upon gradual increase in the concentration of CN^- (0-160 μM) in a DMSO/H_2O (9:1, v/v) solution.

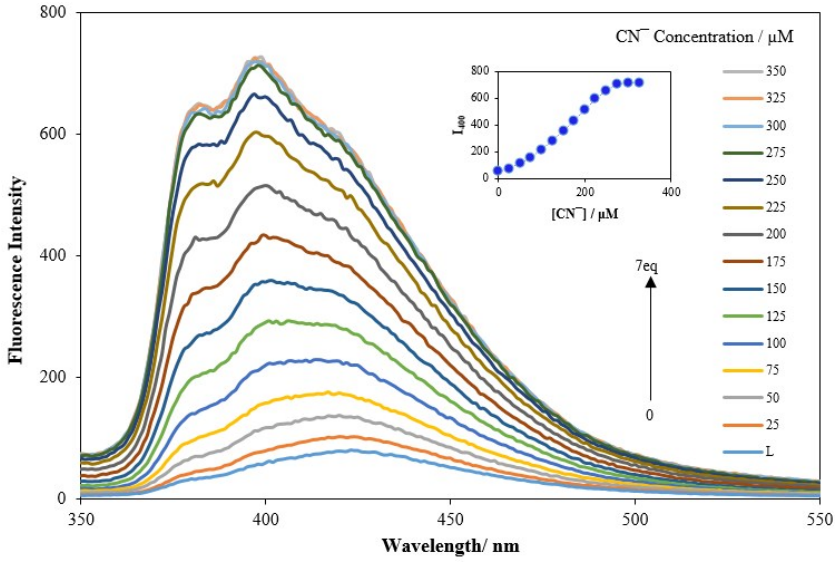

Fig. S4. Changes in the fluorescence spectrum of **L** (30 μM) upon gradual increase in the concentration of CN^- (0−350 μM) in a DMSO/H_2O (9:1, v/v) solution.

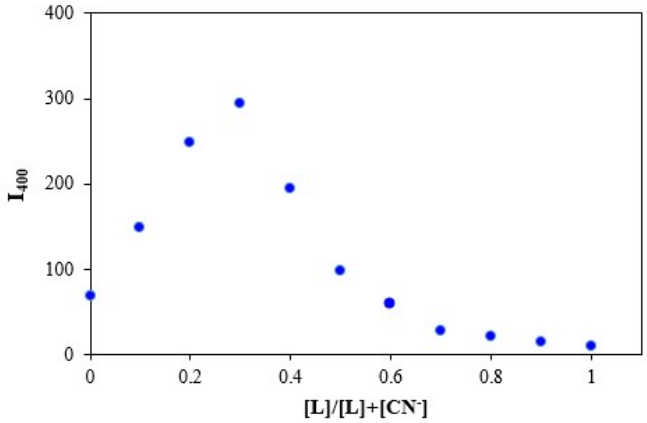

Fig. S5. Job's plot of the complexation between the L and CN^- (λ_{ex} = 340 nm). The total concentration of **L** and CN^- was 100 μM in DMSO solution.

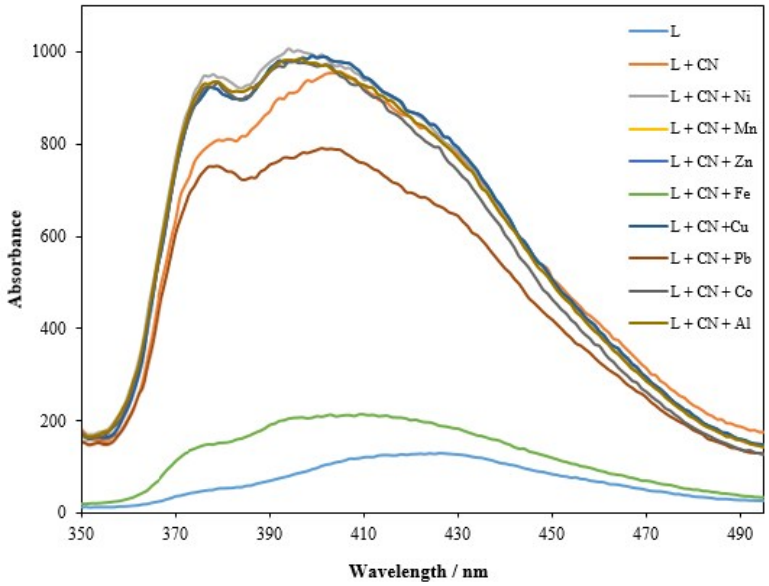

Fig. S6. Changes in the fluorescence spectrum of **L**-CN^- system upon addition of different metal ions in DMSO solution.

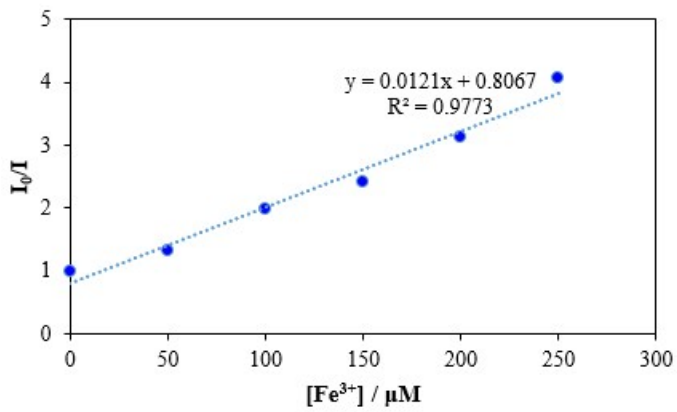

Fig. S7. Stern–Volmer plot of fluorescence quenching of the L-CN^- by Fe^{3+} in DMSO solution.

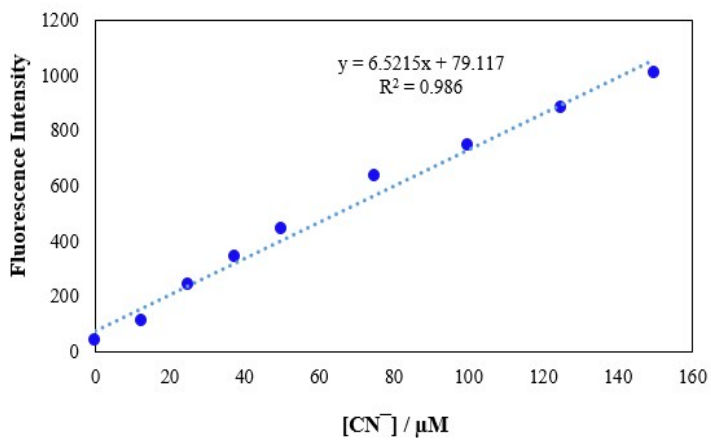

Fig. S8. The fluorescence spectrum linear range of **L-**CN^- at 400 nm upon addition of CN^- in DMSO solution.

Linear Equation: y = 6.5215x + 79.117 R = 0.986

m = 6.5215 $S_b = \sqrt{\frac{\Sigma(F-\bar{F})2}{(N-1)}} = 0.55$ (N = 7)

LOD = $3S_b$ /m

= 2.5×10^{-7} M

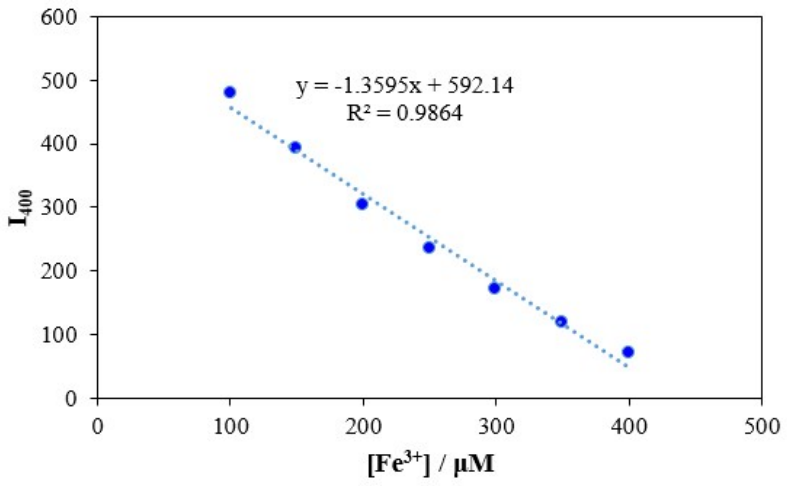

LOD = $3S_b/m$

$= 1.2 \times 10^{-6}$ M

Fig. S9. The fluorescence spectrum linear range of **L**-CN-Fe at 400 nm upon addition of Fe^{3+} in DMSO solution.

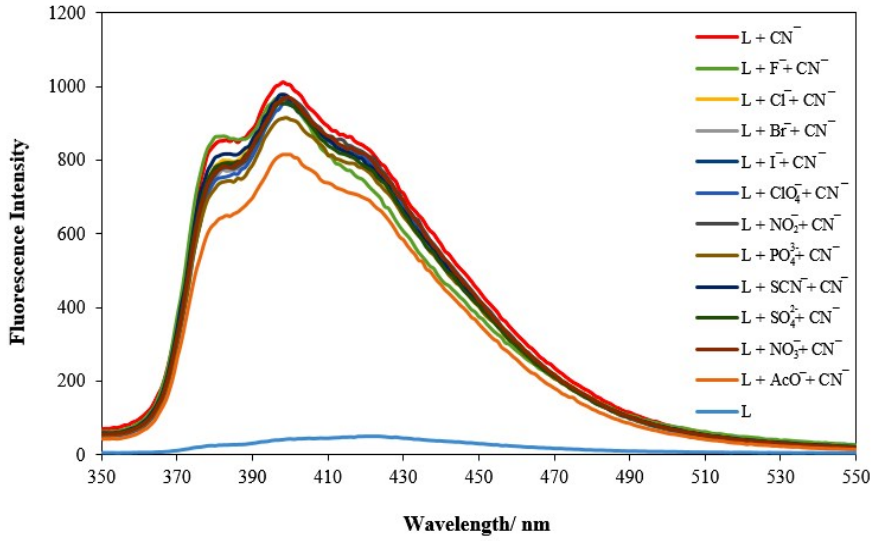

Fig. S10. Changes in the fluorescence intensity of **L**-CN^- in the presence of other interfering anions (150 μM) in DMSO solution.

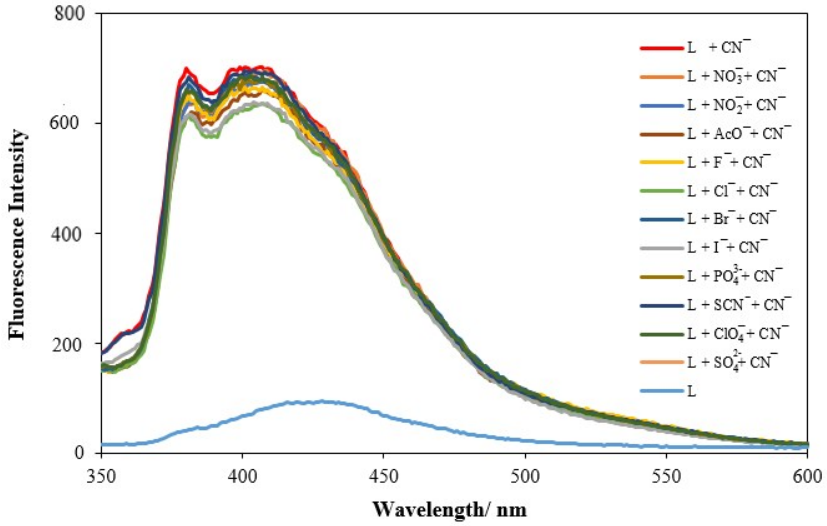

Fig. S11. Changes in the fluorescence intensity of **L**-CN^- in the presence of other interfering anions (350 μM) in DMSO/H_2O (9:1, v/v) solution.

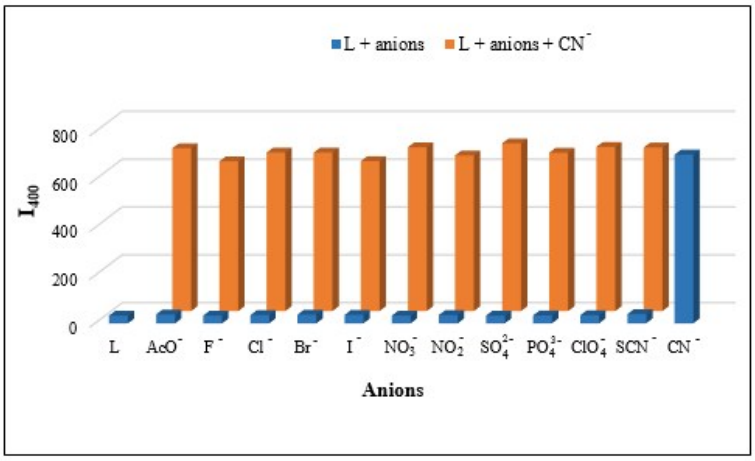

Fig. S12. Competitive selectivity of **L** (5×10^{-5} M) toward CN^- (7 equiv.) in the presence of anions (7 equiv.) with λ_{ex} = 340 nm, slits = 5 nm in DMSO/H_2O (9:1, v/v) solution.

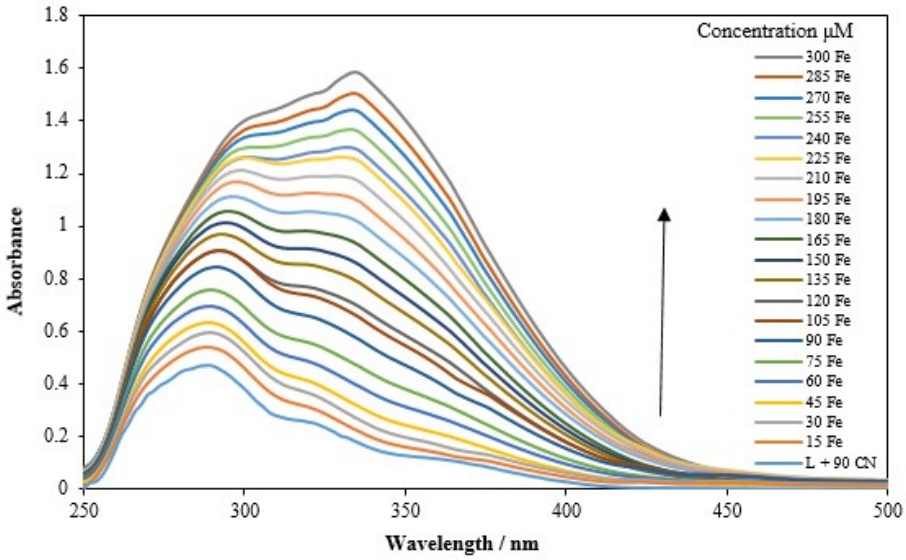

Fig. S13. Changes in the UV-vis spectrum of **L**-CN^- ([**L**] = 3 × 10^{-5} M) system upon gradual increase in the concentration of Fe^{3+} (0-300 μM) in DMSO solution.

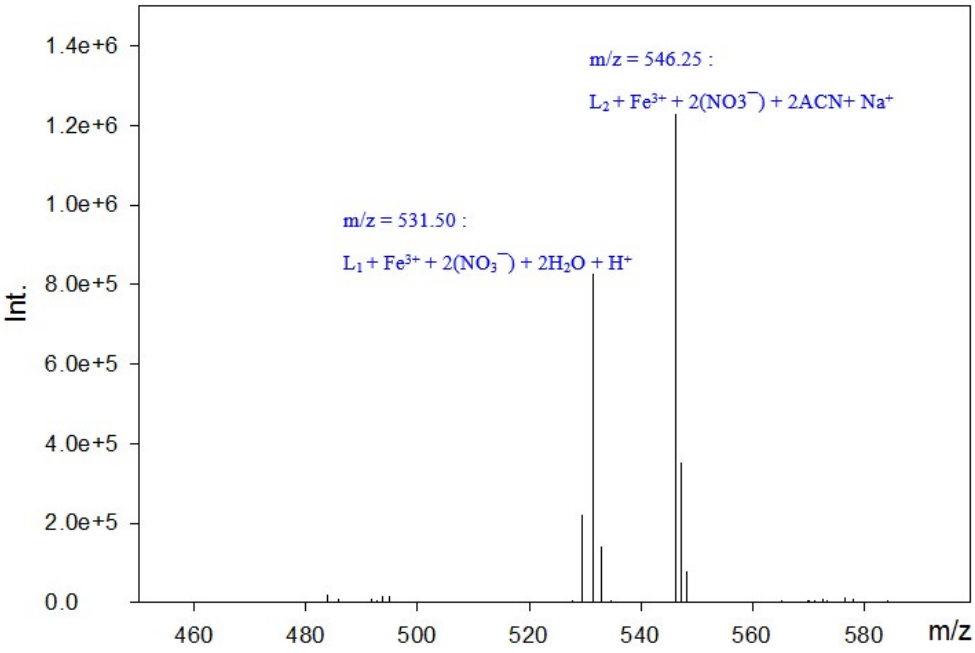

Fig. S14. ESI-MS spectrum for $\mathbf{L_1}$-Fe^{3+} and $\mathbf{L_2}$-Fe^{3+} in DMSO solution diluted by CH_3CN in positive ionization mode.

.

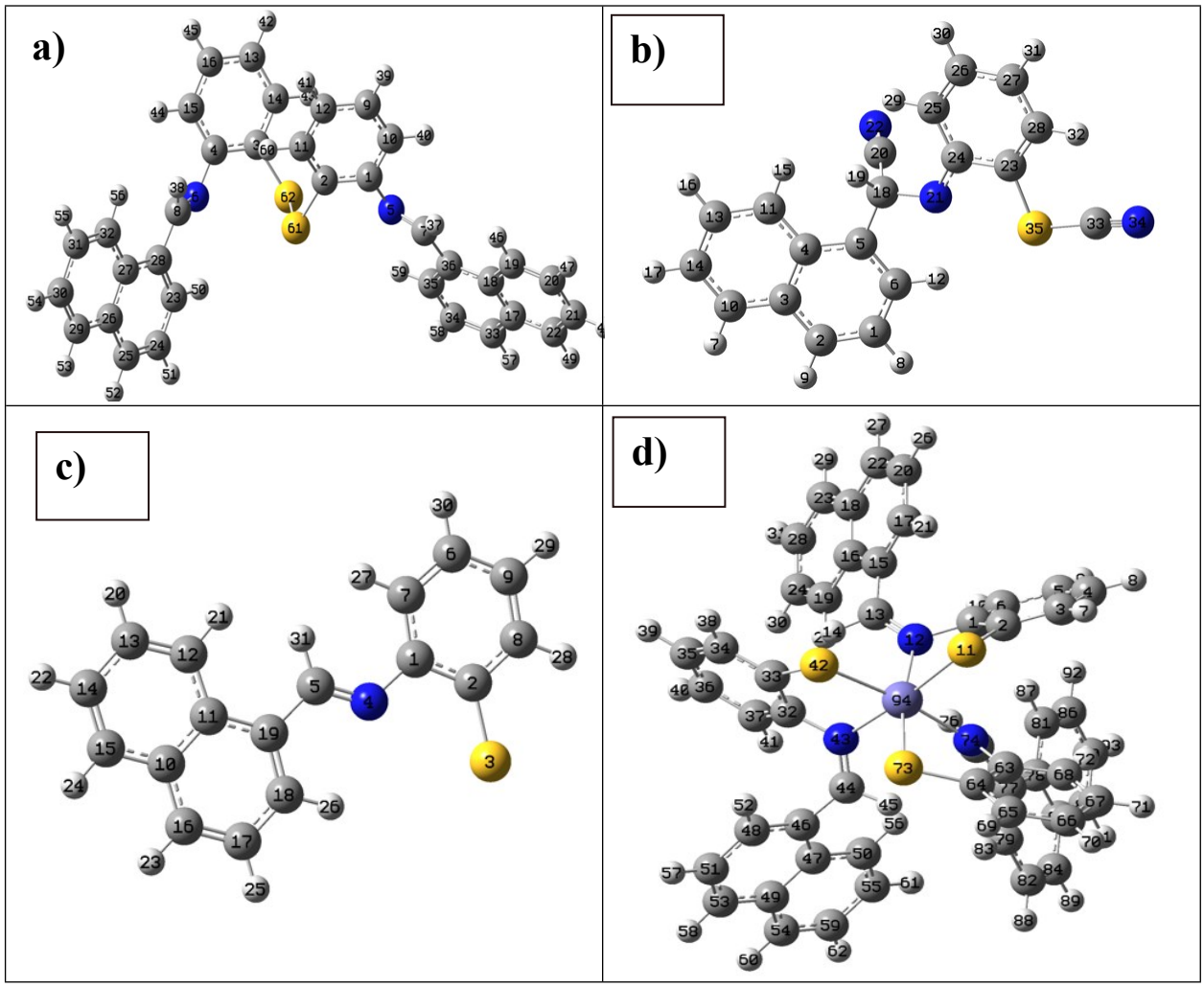

Fig. S15. The optimized structure of **a) L, b) L_1**, **c) L_2** and **d)** [L_2-Fe^{3+}] complex in DMSO solution with atom labelling scheme.

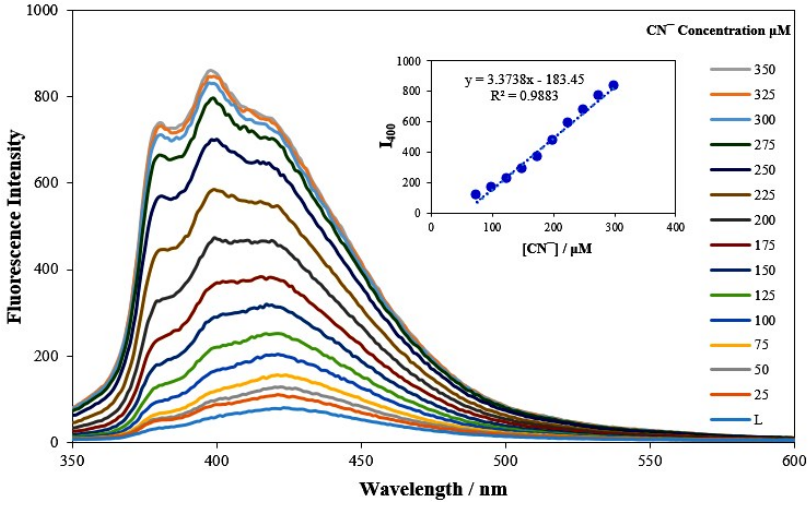

Fig. S16. Changes in the fluorescence intensity of chemosensor **L** (50 μM) upon gradual addition CN^- (0−300 μM) in aqueous solution (λ_{ex} = 340 nm, slits = 5). Inset shows the calibration curve using the fluorescence intensity at 400 nm.

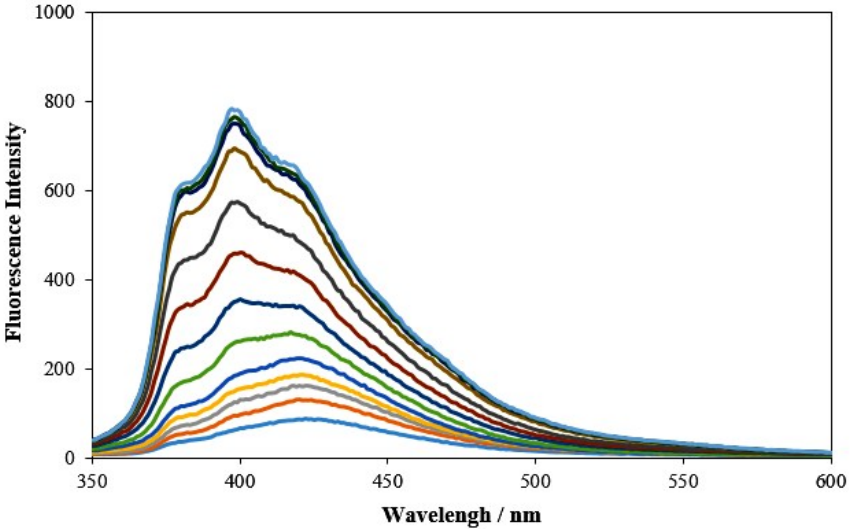

Fig. S17. Changes in the fluorescence intensity of chemosensor **L** (50 μM) upon addition of zinc electroplating wastewater sample, 0-60 μL (λ_{ex} = 340 nm, slits = 5).

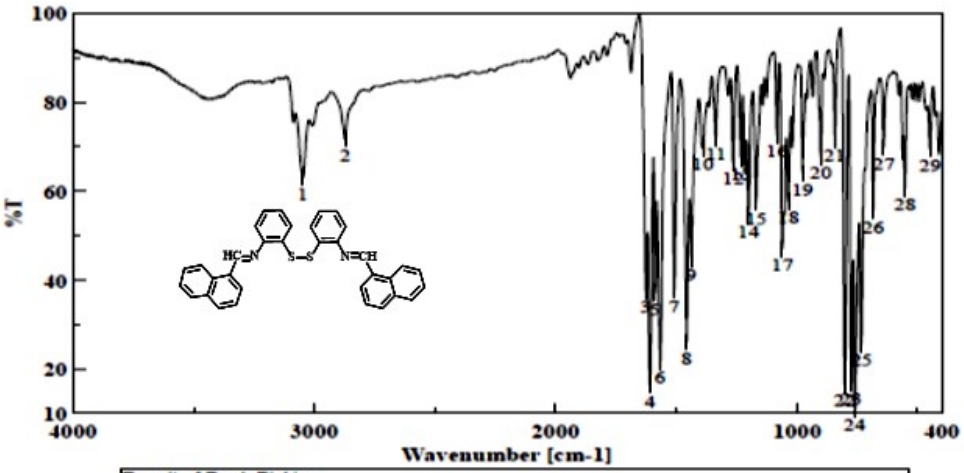

Result of Peak Picking

No.	Position	Intensity	No.	Position	Intensity	No.	Position	Intensity
1:	3046.01	63.0394	2:	2872.45	71.7108	3:	1625.70	37.6480
4:	1608.34	16.4477	5:	1587.13	37.2017	6:	1566.88	21.7977
7:	1508.06	37.8228	8:	1456.96	26.0972	9:	1437.67	44.7845
10:	1390.42	69.6533	11:	1336.43	71.9740	12:	1264.11	66.3654
13:	1232.29	67.3439	14:	1201.43	54.4250	15:	1169.62	57.4431
16:	1082.83	72.6142	17:	1060.66	47.0413	18:	1035.59	57.6455
19:	976.77	64.0329	20:	901.56	67.7857	21:	842.74	71.6634
22:	802.24	16.6349	23:	775.24	16.8735	24:	759.82	11.0610
25:	732.82	25.6259	26:	684.61	55.6181	27:	641.22	69.8636
28:	552.51	60.6423	29:	448.37	69.4197			

Fig. S18. FT-IR spectrum of the **L** as KBr pellet.

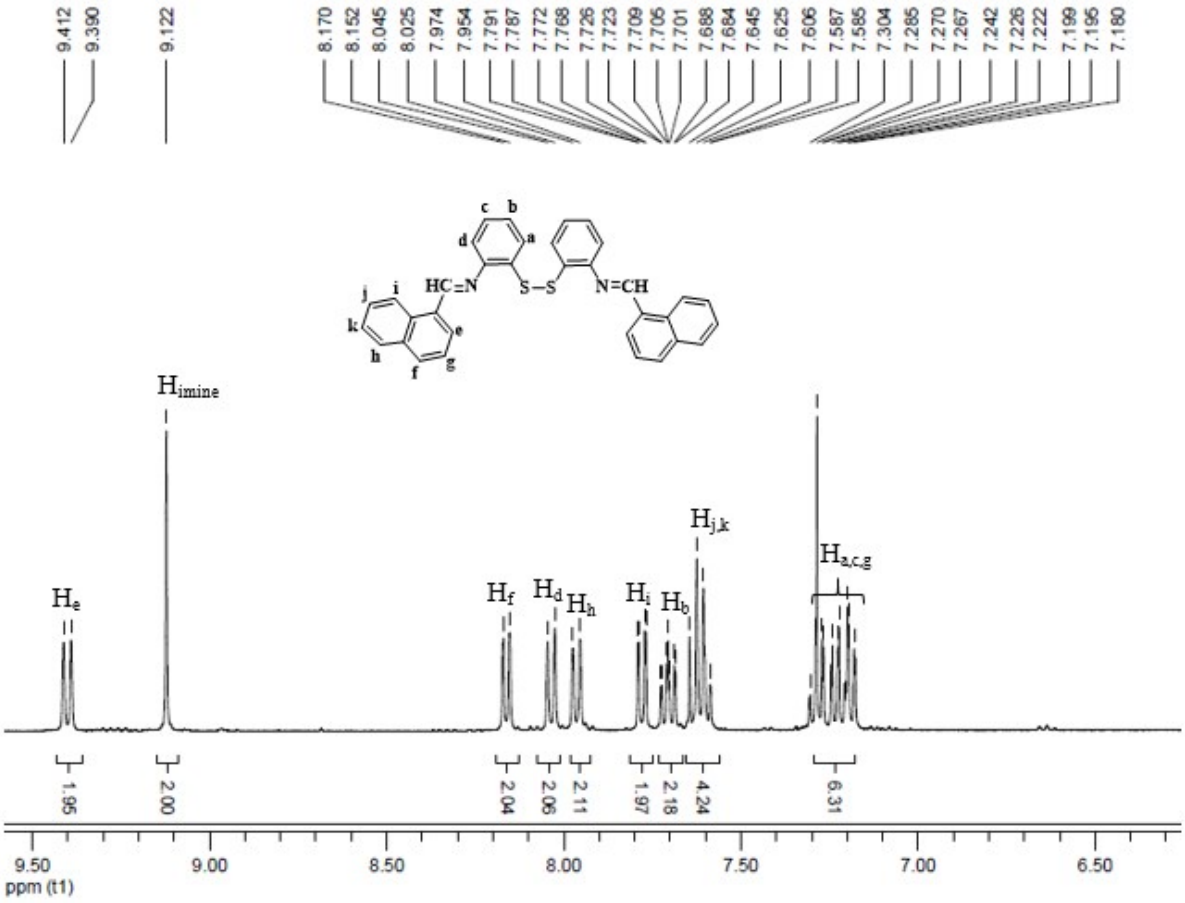

Fig. S19. ^{1}H NMR spectrum of the chemosensor **L** in DMSO-d_6 at room temperature.

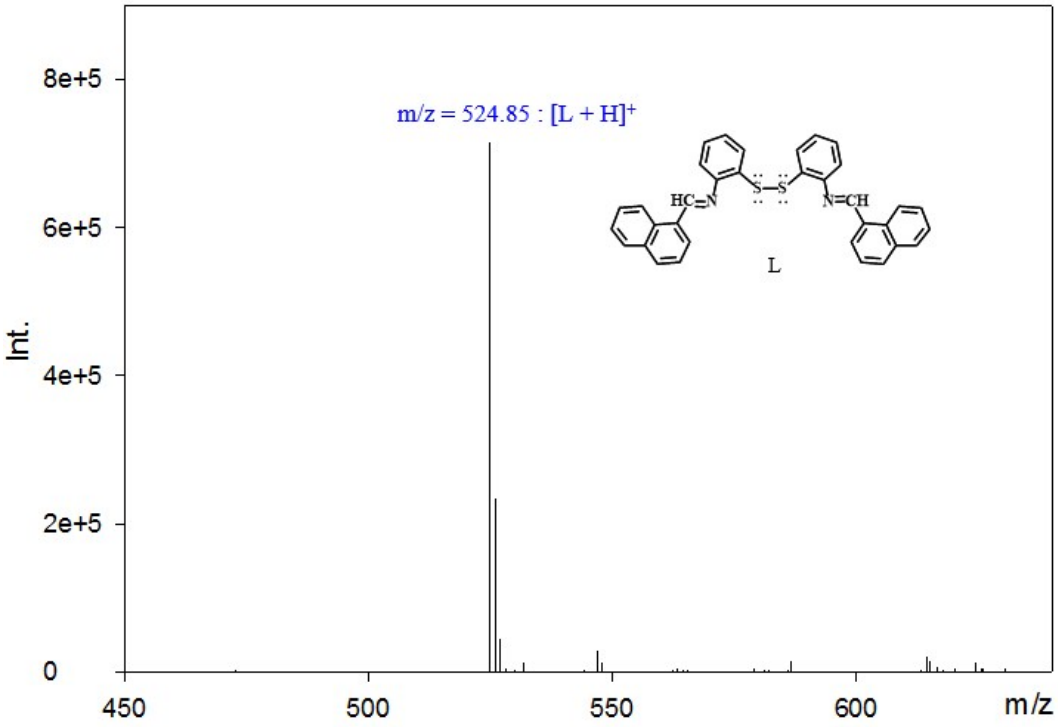

Fig. S20. ESI-MS spectrum of **L** in DMSO solution diluted by CH_3CN in positive ionization mode.

Table S1. Selected bond lengths (Å) and bond angles (º) for chemosensor **L**.

		Bond lengths		
S(1)-S(2)	2.0317(11)	N(1)-C(11)	1.276(3)	1.276(3)
S(1)-C(17)	1.778(2)	N(1)-C(12)		1.421(3)
S(2)-C(18)	1.783(2)	N(2)-C(24)		1.252(3)
N(2)-C(23)	1.418(3)			
		Bond angles		
C(17)-S(1)-S(2)	105.84(8)	C(28)-C(29)-C(34)		119.4(3)
C(18)-S(2)-S(1)	105.37(8)	C(30)-C(29)-C(34)		119.6(3)
C(11)-N(1)-C(12)	120.2(2)	C(9)-C(10)-C(1)	119.3(2)	119.3(2)
C(24)-N(2)-C(23)	121.1(2)	C(9)-C(10)-C(11)		116.0(2)
C(8)-C(7)-C(6)	121.1(3)	C(1)-C(10)-C(11)		124.8(2)
C(8)-C(7)-H(7)	119.5	N(1)-C(11)-C(10)		126.4(2)
C(6)-C(7)-H(7)	119.5	N(1)-C(11)-H(11)		116.8
C(28)-C(29)-C(30)	121.0(3)	C(10)-C(11)-H(11)		116.8
C(17)-S(1)-S(2)-C(18)	92.62(12)			

Table S2.The CMO analysis data of **L**

Structure **L**	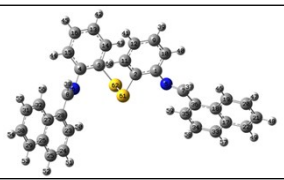	
	NBO	Percent%
LUMO+1	BD*(2) N 6- C 8*	21.2
	BD*(2) C23- C28*	18
	BD*(2) C24- C25*	13.5
	BD*(2) C31- C32*	6.6
	BD*(2) C29- C30*	5.5
LUMO	BD*(2) N 5- C 7*	22
	BD*(2) C35- C36*	16.5
	BD*(2) C33- C34*	11.2
	BD*(2) S61- S62*	8.3
	BD*(2) C 1- C 2*	6.2
	BD*(2) C 9- C12*	5
HOMO-2	LP (2) S61(lp)	29.5
	LP (2) S62(lp)	24

LP: Laon pair , BD: Bonding , BD*: Antibonding

Table S3. The CMO analysis data of $\mathbf{L_1}$

Structure $\mathbf{L_1}$	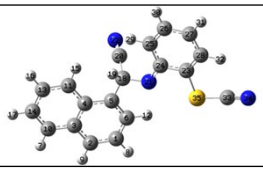	
	NBO	Percent%
LUMO	BD*(2) C11- C13*	24
	BD*(2) C 1- C 2*	22.2
	BD*(2) C 5- C 6*	20.7
	BD*(2) C10- C14*	20.2
HOMO-1	BD (2) C 1- C 2	25
	BD (2) C 5- C 6	24.6
	BD (2) C11- C13	22.3
	BD (2) C10- C14	21.2

Table S4. The CMO analysis data of $\mathbf{L_2}$

Structure $\mathbf{L_2}$	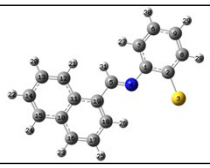	
	NBO	Percent%
LUMO+1	BD*(2) C12- C13*	25
	BD*(2) C14- C15*	20.8
	BD*(2) N 4- C 5*	12.4
	BD*(2) C16- C17*	6.9
	BD*(2) C 8- C 9*	6.8
LUMO	BD*(2) N 4- C 5*	28
	BD*(2) C18- C19*	20.5
	BD*(2) C16- C17*	13.4
	BD*(2) C12- C13*	6
	BD*(2) C 8- C 9*	6
	BD*(2) C14- C15*	5.4
HOMO	LP (3) S3 (lp)	60.9
	BD (2) C 1- C 2	10.8
	BD (2) C 6- C 7	6.3
	BD*(2) C 8- C 9*	5.3

Table S5. The CMO analysis data of $\mathbf{L_2}$-Fe^{3+}

Structure $\mathbf{L_2}$-Fe^{3+}	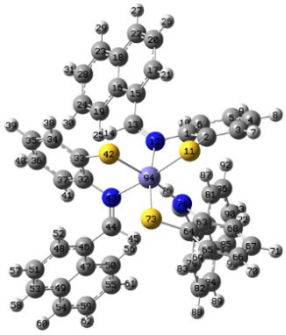	
	NBO	Percent%
LUMO+3	BD*(1) S73-Fe94*	29.6
	BD*(1) S11-Fe94*	9.6
	BD*(2) C15- C17*	6.5
	BD*(1) S42-Fe94*	5.5
LUMO	BD*(2) N74- C75*	24.8
	BD*(2) C77- C79*	11
	BD*(1) S73-Fe94*	8
	BD*(2) C82- C84*	7.4
	BD*(2) N12- C13*	6.3
HOMO	LP (2) S42(lp)	32.4
	LP (2) S11(lp)	22
	BD (2) C32- C33	6
	LP (2) S73(lp)	5

X-ray crystal structure determination

Yellow crystals of the chemosensor **L** suitable for X-ray crystallography were obtained by slow evaporation of an ethylacetate solution of **L** at room temperature. X-ray data for single crystal of **L** was collected on a STOE IPDS-II diffractometer with graphite monochromated Mo-Kα radiation (λ = 0.71073 Å). Data were collected at 298(2) K in a series of ω scans in 1° oscillations and integrated using the Stöe X-AREA [1] software package. The data were corrected for Lorentz and Polarizing effects. The structures were solved by direct methods using SIR2004 [2]. The non-hydrogen atoms were refined anisotropically by the full-matrix least-squares method on F^2 using the SHELXL program [3]. All the hydrogen (H) atoms were introduced in calculated positions and constrained to ride on their parent atoms. Crystallographic data for **L** are listed in Table S6. CCDC 1884337 contains the supplementary crystallographic data for this paper. These data can be obtained free of charge from The Cambridge Crystallographic Data Centre via www.ccdc.cam.ac.uk/data_request/cif.

[1] X-AREA, version 1.30, program for the acquisition and analysis of data, Stoe & Cie GmbH, Darmstadt, Germany, 2005.

[2] M.C. Burla, R. Caliandro, M. Camalli, B. Carrozzini, G.L. Cascarano, L. De Caro, C. Giacovazzo, G. Polidori and R. Spagna, *J. Appl. Crystallogr*., 2005, **38**, 381.

[3] G. M. Sheldrick, *Acta Crystallogr., Sect. A*, 2008, **64**,112.

Table S6. Crystal data and structure refinement for chemosensor **L**

Chemosensor **L**	
Chemical formula	$C_{34}H_{24}N_2S_2$
M_r	524.67
T(K)	298(2)
λ (Å)	0.71073
Crystal system, space group	Triclinic, $P\bar{1}$
a (Å)	7.8343(16)
b (Å)	12.119(2)
c (Å)	14.315(3)
α (°)	85.66(3)
β (°)	78.01(3)
γ (°)	79.57(3)
V(Å^3)	1306.5(5)
Z, Calculated density	2, 1.334 Mg/m^3
μ (mm^{-1})	0.231
F(000)	548
Radiation type	Mo Kα
Crystal size (mm)	0.30 × 0.27 × 0.09
Diffractometer	Stoe IPDS-II
No. of measured, independent and observed [$I > 2\sigma(I)$] reflections	10372, 4500, 2714
R_{int}	0.062
(sin θ/λ)max (Å−1)	0.595
Refinement method	Full-matrix least-squares on F^2
R[F2 > 2σ(F2)], wR(F2), S	0.040, 0.092, 0.81
Goodness-of-fit on F^2	0.812
Final R indices [I>2σ (I)]	R1 = 0.0397, wR2 = 0.0865
R indices (all data)	R1 = 0.0713, wR2 = 0.0923
No. of reflections	4500
No. of parameters	343
H-atom treatment	H-atom parameters constrained
$\Delta\rho_{max}$, $\Delta\rho_{min}$ (e Å^{-3})	0.161, -0.193